Moment T-matrix approach to e^+-H scattering. II. Elastic scattering and total cross section at intermediate energies

Jeremy R. Winick* and William P. Reinhardt

Department of Chemistry, University of Colorado and Joint Institute for Laboratory Astrophysics, University of Colorado and National Bureau of Standards, Boulder, Colorado 80309

(Received 27 March 1978)

Elastic amplitudes for e^+-H scattering are calculated for positron energies from 0.25–1.15 a.u. (~7–34 eV), an energy range where pickup and impact-ionization channels are open. These amplitudes are used to calculate the elastic e^+-H cross section, and assuming unitarity, the total e^+-H scattering cross section.

I. INTRODUCTION

The problem of impact ionization of atoms by charged particles is enormously challenging: not only is there a continuum of open channels, but the long-range nature of the interaction makes even specification of the proper asymptotic form of the wave function a difficult problem.[1] Recently, several groups[2-8] have suggested methods by which at least the elastic cross section and ordinary bound-bound inelastic cross sections may be calculated at energies where the breakup channel is open, but where the energy is not high enough to allow confident use of high-energy approximations. Schlessinger[2] and Nuttall[3,4] (see also[9] T-matrix I) and co-workers have used rational fraction and extrapolation methods to continue the approximate discretized off-shell T matrix

$$T_k(z) = \langle k|V|k\rangle + \langle k|V[1/(z-\bar{H})]V|k\rangle \tag{1.1}$$

from regions of the complex z plane, away from the real axis, where the representation of Eq. (1.1) might be expected to be valid, to take the $z \to E + i\epsilon$ limit needed to extract scattering information. Schlessinger[2] and Nuttall and Cohen[3] have developed use of the technique for short-range potentials, such as in neutron-deutron scattering, while Doolen, Nuttall, and co-workers[4] have applied it to e^--H and e^+-H s-wave elastic scattering above the ionization threshold. Rescigno and Reinhardt[5] have applied related Fredholm techniques to find singlet e^- – H elastic scattering amplitudes above the ionization threshold. Burke and Mitchell[6] and Callaway and co-workers[7] have used pseudostate close-coupling methods in successful e^- – H intermediate-energy investigations. A review on intermediate-energy techniques by Bransden and McDowell[8] has recently appeared.

It is the purpose of this paper to present results for e^+ – H scattering in the intermediate-energy range, just above the ionization threshold. In this region normal pseudostate close-coupling techniques converge much too slowly in the e^+ – H problem to be used conveniently, and, as discussed in T-matrix I,[9] and by Winick,[10] attempts to use the T-matrix extrapolation techniques failed for partial waves higher than $l=0$, as the extrapolation error was similar in size to the desired amplitude. The Fredholm-analytic continuation techniques of Rescigno and Reinhardt,[5] also failed to give reliable higher partial-wave results when applied to e^+ – H scattering. It was thus concluded that convergence in the complex plane of $T_k(z)$ was too poor to allow reliable results in the $z \to E + i\epsilon$ limit to be found by continuation or extrapolation, and that a method using the representation

$$\begin{aligned} T_k(z) &= \langle k|V|k\rangle + \langle k|V[1/(z-\bar{H})]V|k\rangle \\ &= \langle k|V|k\rangle + \sum_i \frac{\langle k|V|\tilde{\chi}_i\rangle\langle\tilde{\chi}_i|V|k\rangle}{z-\tilde{E}_i} \\ &= \langle k|V|k\rangle + \sum_i \frac{\tilde{\rho}_k(\tilde{E}_i)}{z-\tilde{E}_i}, \end{aligned} \tag{1.2a}$$

where

$$\tilde{\rho}_k(\tilde{E}_i) \equiv |\langle k|V|\tilde{\chi}_i\rangle|^2 \tag{1.2b}$$

would have to be developed which calculated T_k $(E + i\epsilon)$ directly. This was accomplished in T-matrix I (Ref. 9) by using the raw distribution $\tilde{\rho}_k(\tilde{E}_i)$ to find the discontinuity of $T_k(z)$ across the cuts on the real axis, followed by a dispersion calculation of $T_k(E+i\epsilon)$, itself, from the discontinuity via a Hilbert transform. The principal advantages of this method are that boundary conditions need not be explicitly enforced and that the difficult parts of the calculation may be performed in a correlated Hylleraas-type basis, using L^2 functions and standard matrix techniques. Correlation and polarization are so important in e^+ – H scattering (as opposed to the e^- – H case) that use of correlated basis functions is almost a necessity for obtaining even moderately accurate results.

The reader is referred to T-matrix I for a detailed description of the calculation of $T_k(E+i\epsilon)$ from the discretized representation of Eq. (1.2a),

and for references to the $e^+ - H$ theoretical literature. In this paper we present the results of applying the method to the calculation of the $e^+ - H$ elastic cross section, and, utilizing unitarity, the $e^+ - H$ total scattering cross section over the energy region 0.25–1.25 a.u. (~6.8–~34 eV). These results are presented in Sec. II followed by a discussion in Sec. III.

II. ELASTIC e^+-H SCATTERING

We summarize the results of calculation of partial-wave amplitudes in Sec. II A, followed by the resulting elastic and total cross sections.

A. Partial-wave amplitudes

1. s waves

The s-wave amplitude is a crucial test of the method, as it is the only partial wave for which reliable previous results exist above the ionization threshold. Calculations were carried out with basis functions of the type

$$\phi_i(\vec{r}_1,\vec{r}_2) = r_1^{n_1} r_2^{n_2} r_{12}^{n_{12}} \exp(-\alpha r_1 - \beta r_2) \times \mathcal{Y}_{l_1,l_2,L=0}(\hat{\Omega}_1,\hat{\Omega}_2), \quad (2.1)$$

where $\vec{r}_1$ denotes the (vector) coordinate of the electron, and the $\vec{r}_2$ is the corresponding positron coordinate. As in T-matrix I, the static channel was defined by setting $\alpha = 1.0$, and including functions with $n_1 = 0$, $n_{12} = 0$, $n_2 = 0, 1, 2, 3, \ldots$. Calculations with n_1, n_2, n_{12} chosen such that all combinations with $M \equiv n_1 + n_2 + n_{12} \leq 5$ (56 terms), $M \leq 6$ (84 terms) were carried out, yielding reasonable, but not fully converged results. Extending the calculation to include all terms with $M \leq 7$ was not feasible without substantial modification of the programs: a final 105-term calculation including all $M \leq 6$ terms and most of the $M = 7$ terms yielded the results of Table I for $\beta = 0.7$, 0.8, and 0.9; these are compared with the extrapolation results of Doolen and Nuttall. Agreement is quite satisfactory over the range $k = 0.8 - 1.5$ a.u.. The resulting elastic cross section is shown in Fig. 1.

A further test is possible in the inelastic region.

TABLE I. s-wave elastic amplitudes in the inelastic region. A, B, and C are results obtained from eight-point quadratures from 16 moments of $x = (E-S2)/(E+S2)$ for at least five different mappings, and thus at least five sets of results for each k and β. Column D represents the results of Doolen *et al.* (Ref. 4).

	A		B	
	105S $\alpha=1$ $\beta=0.8$		105S $\alpha=1$ $\beta=0.9$	
k (a.u.)	Ret	Imt	Ret	Imt
0.8	−0.098(1)[a]	0.013[b]	−0.097(1)	0.0133
0.9	−0.135(1)	0.026	−0.136(1)	0.026
1.0	−0.165(1)	0.046	−0.166(1)	0.043
1.1	−0.195(2)	0.065	−0.1894(11)	0.065
1.2	−0.216(3)	0.080	−0.2133(25)	0.087
1.3	−0.226(2)	0.101(5)	−0.234(3)	0.102(5)
1.4	−0.238(3)	0.130(10)	−0.245(3)	0.117(3)
1.5	−0.255(4)	0.155(20)	−0.250(3)	0.140(10)

	C		D	
	105S $\alpha=1$ $\beta=0.7$			
k (a.u.)	Ret	Imt	Ret	Imt
0.8	−0.0998(6)	0.013	−0.098	0.014
0.9	−0.1389(9)	0.027	−0.143	0.020
1.0	−0.1706(12)	0.045	−0.174	0.03
1.1	−0.1950(20)	0.062	−0.201	0.05
1.2	−0.211(2)	0.087	−0.22	0.07
1.3	−0.233(7)	0.115(7)	−0.240	0.09
1.4	−0.260(6)	0.147(15)	−0.25	0.10
1.5	−0.284(5)	0.158(15)	−0.28	0.12

[a] The number in parenthesis is the standard deviation of the values. It applies to the last places in the amplitude. For example, −0.216(3) means −0.216 ± 0.003.

[b] When not indicated, probable uncertainty in the imaginary part is less than or equal to ±5%. Error for the real part is the standard deviation of the spread of the values obtained from different mappings.

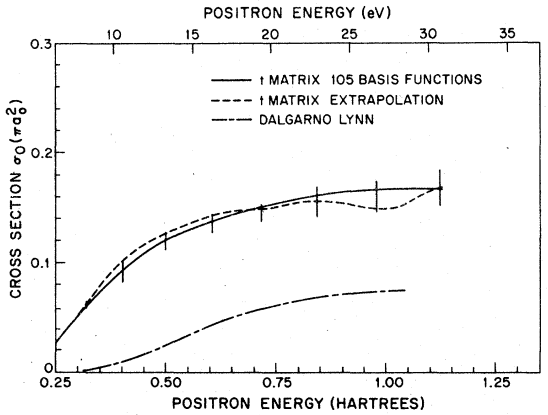

FIG. 1. Elastic s-wave partial cross section above the positronium pickup threshold. The elastic partial cross section is indicated by the solid line. The error bars indicate deviations obtained from moment T-matrix calculations using 105 basis functions and $\beta = 0.7$, 0.8, and 0.9 using 16 moments and eight-point quadrature. The dashed curve are results of T-matrix extrapolations using up to 120 basis functions (Ref. 4). The broken curve (— - —) is obtained from the adiabatic Dalgarno-Lynn potential.

Between the pickup threshold at a positron energy of 0.25 a.u. and the $1s-2s, 2p$ excitation threshold at 0.375 a.u. only two channels are open: purely elastic scattering and positronium formation. Numerous calculations of varying degrees of sophistication have been carried out in this energy range. The nonlocal two-channel close-coupling equations for the elastic and pickup channels (referred to as the coupled static approximation) were solved by Bransden and Jundi,[11] and a simplified separable formulation by Fels and Mittleman,[12] giving substantially different results.

TABLE II. s-wave elastic positron-hydrogen amplitudes comparison of various methods at $k = 0.8$.

	Ret	Imt
Moment T matrix	-0.098 ± 0.002	0.013 ± 0.0005
Nuttall[a]	−0.098	0.014
Fraser[b]	−0.109	0.0125
Dirks and Hahn[c]	−0.155	0.025
Coupled Static[d]	−0.309	0.108
Stein[e]	−0.104	0.011
Wakid[f]	−0.241	0.062

[a] T-matrix extrapolation technique of Ref. 4.
[b] Coupled static plus L^2 correlation functions of the Hylleraas type of Ref. 17.
[c] Generalized variational bound formulation of Ref. 13.
[d] See Ref. 11 or 17.
[e] Kohn and Hulthen variational methods of Ref. 16.
[f] Algebraic close-coupling approximation. The authors' approximation (e) of Ref. 15.

Both of these two-state approximations have been complemented by the addition of polarization potentials, although in a nonvariational manner. Again the two calculations give differing results. There have been several attempts at systematic variational calculations in the inelastic region between the pickup and $n = 2$ thresholds. The two open channels can be explicitly included, and complemented with square integrable correlation functions to represent polarization and correlation due to closed channels. In approximate chronological order, Dirks and Hahn[13]; Seiler, Oberoi, and Callaway[14]; Wakid and LaBahn[15]; Stein and Sternlicht[16]; and Chan and Fraser[17] have calculated variationally corrected amplitudes in this two-channel region, with either Slater-type or Hylleraas-type basis functions. The results at $k = 0.8$ a.u. are summarized in Table II where they are compared with the T-matrix extrapolation results of Doolen *et al.*[4] and with the present moment T-matrix result. The results are again seen to be satisfactory, giving the confidence needed to extend the calculations to higher partial waves, where relatively little is known about the amplitudes.

2. *p-wave amplitude*

The distinguishability of the electron and positron implies that correlation and polarization will probably play a more important role in $e^+ - \mathrm{H}$ scattering than in $e^- - \mathrm{H}$ scattering as in the $e^+ - \mathrm{H}$ case the Pauli principle does not prevent the positron from entering the region near the nucleus. A manifestation of this becomes apparent in considering the functions

$$\mathcal{Y}_{l_1, l_2, L=1}(\hat{\Omega}_1, \hat{\Omega}_2), \tag{2.2}$$

where we now must include $l_1 = 0$, $l_2 = 1$ *and* $l_2 = 1$, $l_2 = 0$ terms. In the $e^- - \mathrm{H}$ case, appropriate symmetrization of the basis would allow inclusion of only one of these couplings, as the electrons are identical. Thus for a given value of $M = n_1 + n_2 + n_{12}$ the basis

$$\phi_i(\vec{r}_1, \vec{r}_2) = r_1^{n_1} r_2^{n_2} r_{12}^{n_{12}} \exp(-\alpha r_1 - \beta r_2)\, \mathcal{Y}_{l_1, l_2, L=1}(\hat{\Omega}_1, \hat{\Omega}_2) \tag{2.3}$$

will have twice the size of the corresponding $e^- - \mathrm{H}$ basis. This implies that much less radial (r_1, r_2) and interparticle (r_{12}) nodal structure can be described for a fixed basis size.

The present calculations were carried out using 45, 56, and 87 basis functions. Again all functions satisfying a given M were not included. Functions with either high powers of r_1 or r_2, especially terms that have high powers of r_2 with the coupling $l_1 = 1$, $l_2 = 0$ were left out.

TABLE III. p-wave elastic amplitudes in the inelastic region.[a]

k (a.u.)	A: 87P $\alpha=1$ $\beta=0.7$ Ret	A: Imt	B: 87P $\alpha=1$ $\beta=0.8$ Ret	B: Imt
0.8	0.163(6)[b]	0.055[c]	0.161(2)	0.055
0.9	0.154(2)	0.068	0.152(5)	0.066
1.0	0.133(3)	0.083	0.133(2)	0.076
1.1	0.109(5)	0.089	0.113(3)	0.093
1.2	0.088(5)	0.093	0.077(1)	0.099
1.3	0.055(3)	0.101	0.052(1)	0.092
1.4	0.030(6)	0.118(5)	0.034(7)	0.119
1.5	(c)	(c)	0.007(3)	0.141(20)

k (a.u.)	C: 87P $\alpha=1$ $\beta=0.6$ Ret	C: Imt	D: 87P $\alpha=1$ $\beta=0.9$ Ret	D: Imt
0.8	0.158(1)	0.056		
0.9	0.143(2)	0.070		
1.0	0.120(2)	0.080		
1.1	0.093(4)	0.089	0.118(7)	0.090
1.2	0.066(4)	0.088	0.083(4)	0.106
1.3	0.049(7)	0.099	0.043(4)	0.102
1.4	(c)	0.110(15)	0.025(4)	0.098
1.5	−0.018(8)	0.105	0.014(2)	0.118

[a] The results in A, B, C, and D are from 87 p-wave T-matrix calculations using eight-point quadratures from 16 moments of $x=(E-S2)/(E+S2)$. At least five different values of $S2$ are used giving at least five values of real t for each k and β. Missing values, indicated by (c), indicate that the large range of values made the answer unreliable.

[b] See Table I.

[c] When not indicated, probable uncertainty in the imaginary part is less than or equal to ± 5%. Error for the real part is the standard deviation of the spread of the values obtained from different mappings.

The calculated amplitudes are tabulated in Table III for the four choices of the nonlinear parameter $\beta=0.6$, 0.7, 0.8, and 0.9. The real parts are an average of the dispersion-corrected results of different eight-point quadratures which correspond to different mapping parameters $S2$ (see T matrix I). The results for the high momenta $k=1.3$, 1.4, and 1.5 are somewhat disappointing. There is a considerable deviation arising from calculations with the same β and different mappings. This error is not that important for the very small real part since it does not affect the cross section very much. However, the imaginary part is also uncertain since the points obtained from different mappings do not all fall on or very near a single line. The value of the imaginary part seems to depend upon the value of $S2$; the higher values of $S2$ generally give curves that would give larger imaginary parts. The values of the imaginary parts also vary with the choice of β and the difference between the different results is often larger than the spread for calculations using the same β but different $S2$. This indicates that the calculation is somewhat basis set dependent. It would be hoped that this basis set dependence would become less noticeable for larger basis sets. However, little improvement in this respect was noticed in going from 56 to 87 basis functions. The partial cross section is shown in Fig. 2. The uncertainties introduce error "bars" of relatively large size. Chan and McEachran[18] have calculated the p-wave elastic amplitude for energies between pick-up and the $n=2$ thresholds using a 50-term configuration interaction (no interparticle coordinates) wave function. As their partial cross-section results in the region below the pick-up threshold are 10%–15% below the converged results of Bhatia *et al.*,[19] it is clear that the CI basis is not sufficient to fully describe correlation, making comparison difficult in the two-channel region: we simply note that their result is about 12% lower than ours at $k=0.8$.

3. *Higher partial waves*

The d-wave amplitudes were calculated with 62, 81, and 100 basis functions. The 100 basis function calculations used $\beta=0.6$, 0.7, and 0.8. For the d-wave case there are now three $l+1$, differ-

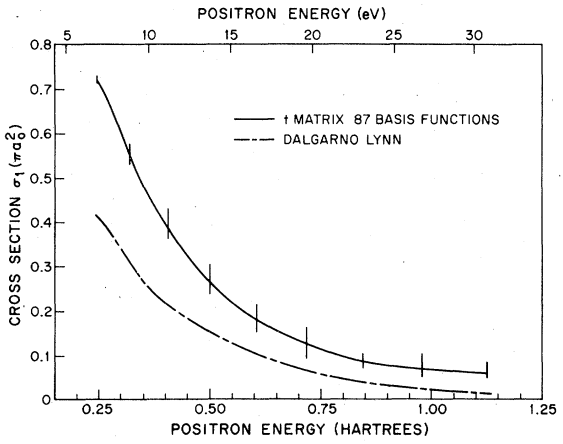

FIG. 2. p-wave elastic partial cross section in the inelastic region. The solid curve is obtained from the moment T-matrix amplitudes of Table III. All the T-matrix calculations used 87 basis functions. The possible error is indicated by the bars. The bars represent the deviation among the different calculations and the uncertainty in Imt which is usually of the order of ± 0.005. The broken curve (— - —) is the cross section obtained using the adiabatic Dalgarno-Lynn approximation (Ref. 20).

TABLE IV. d-wave elastic amplitudes in the inelastic region. [a]

	A		B		C	
	$100D$ $\alpha=1$ $\beta=0.7$		$100D$ $\alpha=1$ $\beta=0.8$		$100D$ $\alpha=1$ $\beta=0.6$	
k (a.u.)	Ret	Imt	Ret	Imt	Ret	Imt
0.8	0.1107(10)[b]	0.033[c]	0.1106(9)	0.036	0.1118(15)	0.034
0.9	0.1193(20)	0.070	0.1087(30)	0.071	0.1136(15)	0.070
1.0	0.1015(10)	0.097	0.0994(11)	0.090	0.0954(24)	0.094
1.1	0.076(2)	0.108	0.0837(20)	0.108	0.0807(26)	0.107
1.2	0.057(4)	0.110	0.0621(23)	0.114	0.0584(49)	0.115
1.25					0.0474(33)	0.115(10)
1.3	0.040(4)	0.107	0.0359(27)	0.107	0.0246(171)	0.115(10)
1.35	0.0308(16)	0.107			0.0025(75)	0.103
1.4	0.020(2)	0.108(8)	0.0213(31)	0.099	0.0143(60)	0.099
1.45	0.0144(11)	0.101			−0.0048(19)	0.093
1.5	0.004(2)	0.097	0.0130(21)	0.097	−0.0064(40)	0.084
1.55	−0.0058(29)	0.092				

[a] All calculations of t_k used an eight-point quadrature obtained from 16 moments of $x=(E-S2)/(E+S2)$. At least five different maps yielding different quadratures are used to obtain different real parts of t for each k and β.

[b] See Table I.

[c] When not indicated, probable uncertainty in the imaginary part is less than or equal to ± 7%.

ent angular moment couplings of the same parity as the initial incoming state of s-state hydrogen and $l=2$ positron. The 100-function calculation includes functions through $M=6$ and powers of r_{12} as high as four; results are displayed in Table IV. The absolute deviations in the real part and the variance between calculations using different β are not any larger than for the s-wave case, but the percentage uncertainty is larger. The uncertainty in the imaginary part is not indicated in the table but is usually between ± 5% and 10%, the larger error generally occurring at higher energies. The d-wave partial cross section is plotted in Fig. 3.

The f-wave amplitudes were calculated using 45 and 76 basis functions. The f-wave problem has four distinct couplings, thus we had about 19 functions for each of these "channels." The 76 functions include most combinations such that $M \leq 6$ including all possible r_{12}^3 terms with this restriction. A few functions with high powers of r_1 are left out such as $r_1^6 r_2^0 r_{12}^0 \exp(-r_1-\beta r_2)$ in the $l_1=3$, $l_2=0$ coupling block which we assume did not contribute as much as the terms retained.

The amplitudes in Table V are now quite small for the entire range of energy, the largest real part being about 0.06 and the largest imaginary part 0.07. The variation between the calculations is quite large, in fact, of the same order as the difference between the 45- and 76-function calculations. The real part of the amplitude seems somewhat dependent upon β especially for $k=1.4$ and 1.5. The f-wave amplitudes represented a particularly bad case for the moment T-matrix method; sample results for $\mathrm{Im}t_k(E+i\epsilon)$ for $k=1.1$ a.u. are shown in Fig. 4 of T-matrix I. There are two possible solutions to this problem. The first is to use a larger basis set in which the raw distribution would hopefully be smoother since it would be more dense. However, including most functions for $M=7$ would mean about 130 functions

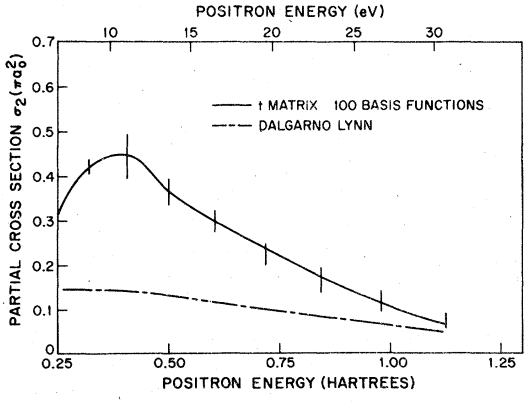

FIG. 3. d-wave elastic partial cross section in the inelastic region. The solid curve represents moment T-matrix results using 100 basis functions. The possible error resulting from deviations arising from the various amplitudes given in Table IV is indicated by the bars. The broken curve (— - —) is the result from the phase shifts in the adiabatic Dalgarno-Lynn approximation.

TABLE V. f-wave elastic amplitudes in the inelastic region.[a]

k (a.u.)	A 76F $\alpha=1$ $\beta=0.7$ Ret	Imt	B 76F $\alpha=1$ $\beta=0.6$ Ret	Imt
0.8	0.0444(11)[b]	0.0051	0.0442(5)	0.0045
0.9	0.0566(15)	0.0255	0.0579(39)	0.0207
1.0	0.0531(6)	0.0488	0.0578(22)	0.0465
1.1	0.0400(10)	0.0564	0.0493(22)	0.0580
1.2	0.0373(10)	0.0585	0.0323(48)	0.0655
1.3	0.0319(23)	0.070	0.0152(16)	0.072
1.4	0.0146(73)	0.071	0.0027(10)	0.062
1.5	−0.0050(36)	0.066	−0.0007(10)	0.055
k (a.u.)	C 76F $\alpha=1$ $\beta=0.7$ Ret	Imt	D 76F $\alpha=1$ $\beta=0.8$ Ret	Imt
0.8	0.0443(4)	0.0055	0.0452(60)	0.0038
0.9	0.0601(17)	0.0245	0.0632(38)	0.0208
1.0	0.0539(50)	0.049	0.0598(18)	0.0530
1.1	0.0398(10)	0.055	0.0394(16)	0.068
1.2	0.0380(12)	0.0575	0.0265(21)	0.0605
1.3	0.0313(110)	0.066	0.0255(15)	0.0575
1.4	0.0196(220)	0.0705	0.0241(7)	0.062
1.5	−0.0035(45)	0.0665	0.0161(20)	0.0671

[a] A and B use eight-point quadratures obtained from 16 moments of $x=(E-S2)/(E+S2)$, while C and D use seven points from the first fourteen moments of $x=(E-S2)/(E+S2)$. At least five different $S2$ are used for each k and β. Probable uncertainty in the imaginary part is less than ± 10%.

[b] See Table I.

which would be too large to be easily incorporated. With a limit of about 110 functions, we would have to choose more carefully which 30 we would add. In any event, this would mean a much more expensive calculation and there would be no guarantee of better behavior. The second choice is to try and use the same information from the 76 functions but to "smooth" it more. We tried a seven-point quadrature which used only fourteen moments in an effort to smooth out the large contributions from some of the individual $\tilde{\rho}_i(\tilde{E}_i)$. The seven-point quadrature seemed to give more consistent results for the imaginary part, but did not help the calculation of the real part, especially for $\beta=0.7$. The f-wave elastic partial cross section is shown in Fig. 4. The errors are estimates from the spread of values shown in Table V. The cross section, as in the d-wave case, is larger than the Dalgarno-Lynn[20] result. The largest departure occurs just above threshold with a peak at about 13–14 eV and by 30 eV our correlated result falls to the Dalgarno-Lynn value. Our results would indicate that for these higher partial waves the long-range polarization force again becomes dominant about 20 eV above the inelastic threshold. The contribution to the total cross section can be seen in Fig. 9. This contribution is again similar to the d-wave case with a peak value of about $1.35\pi a_0^2$ at 14 eV. It is interesting to note that the peak occurs at the impact-ionization

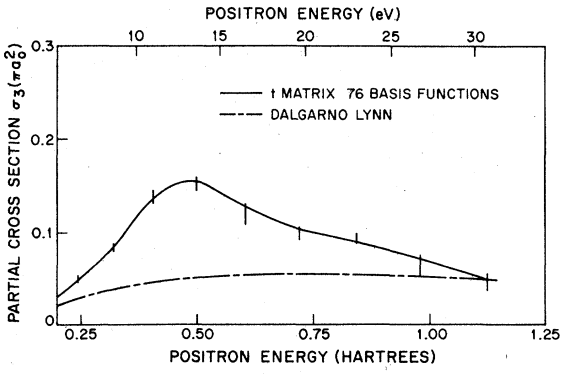

FIG. 4. f-wave elastic partial cross section in the inelastic region. The results are obtained from the moment T-matrix amplitudes of Table V. The deviations in the amplitudes yield the expected errors shown by the error bars on the solid curve. The broken curve (— - —) is calculated from the phase shifts obtained by integrating the radial Schrödinger equation with the Dalgarno-Lynn adiabatic potential.

TABLE VI. g-wave elastic amplitudes in the inelastic region.[a]

k (a.u.)	A 87G $\alpha=1$ $\beta=0.6$ Ret	Imt	B 87G $\alpha=1$ $\beta=0.7$ Ret	Imt
0.8	0.0165	4.6×10^{-4}	0.0165	6.5×10^{-4}
0.9	0.0219(70)[b]	0.0041	0.0251(3)	0.0045
1.0	0.0285(80)	0.017	0.0315(25)	0.017
1.1	0.0271(90)	0.0315	0.0271(5)	0.0265
1.2	0.0181(40)	0.031	0.0176(30)	0.035
1.3	0.0156(60)	0.028	0.0132(26)	0.034
1.4	0.0147(20)	0.040	0.00989(150)	0.029
1.5	0.0070(60)	0.045	0.0171(8)	0.032
k (a.u.)	C 87G $\alpha=1$ $\beta=0.8$ Ret	Imt	D 87G $\alpha=1$ $\beta=0.6$ Ret	Imt
0.8	0.0169	3.7×10^{-4}		
0.9	0.0243(45)	0.0045	0.0240(10)	0.0047
1.0	0.0332(27)	0.0194	0.0314(20)	0.017
1.1	0.0240(10)	0.026	0.0248(20)	0.029
1.2	0.0241(20)	0.031	0.0160(30)	0.0298
1.3	0.0175(43)	0.034	0.0151(14)	0.032
1.4	0.0063(12)	0.035	0.0133(70)	0.038
1.5	0.0071(21)	0.0283	0.0072(20)	0.046

[a] A uses an eight-point quadrature obtained from the first 16 moments of $x=(E-S2)/(E+S2)$ using at least five mappings for each k and β. D uses seven points from the first 14 moments. B and C use (16,8) for $k=0.8$, but (14,7) for $k\geq0.9$. Probable error in the imaginary part is less than 10% usually about ± 5%.

[b] See Table I.

threshold.

The g-wave amplitudes using 87 correlation functions are shown in Table VI. The 87 Hylleraas terms include most functions satisfying $M\leq7$ plus an extra static function and leaving out a few high r_1 and r_2 power terms especially for the couplings other than the $l_1=0$, $l_2=4$. The highest power of r_{12} is r_{12}^3 which should be sufficient to describe g-wave correlation and polarization effects, but which is not a good representation for describing bound-state positronium. We, however, do not expect positronium formation to be a very favorable process for these high partial waves; in fact, two-state plus correlation calculations[16] show that it is even small for s-wave scattering in the region where it is the only inelastic channel open—a region where it is expected to be most favored. The amplitudes now are noticeably smaller than the f-wave case, and we are reaching the limit where the variation in different calculations and a reasonable estimate of errors involved is becoming a large fraction of the amplitude. Fortunately, the partial elastic amplitude (see Fig. 5) is quite small. As may be seen in Fig. 7, it seems likely that the elastic cross section is beginning to converge.

For the $L=5$, h-wave case there are six distinct angular momentum coupling channels and thus we quickly reach quite large expansions. Calculations using 108 correlation terms which

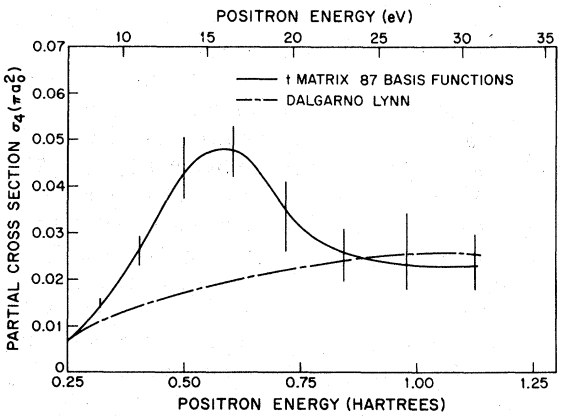

FIG. 5. g-wave elastic partial cross section in the inelastic region. The solid curve gives the moment T-matrix results obtained from the amplitudes in Table VI. The error bars are the expected deviations from the various amplitudes in Table VI. The broken curve (— - —) are results from the phase shifts for the adiabatic Dalgarno-Lynn approximation.

TABLE VII. h-wave elastic amplitudes in the inelastic region.[a]

	A		B		DL
	$108H$ $\alpha=1$ $\beta=1.2$		$108H$ $\alpha=1$ $\beta=0.9$		
k (a.u.)	Ret	Imt	Ret	Imt	Ret
0.8	0.00703(3)[b]	1.66×10^{-4}	0.00741(1)	1.11×10^{-4}	0.0075
0.9	0.0106(1)	1×10^{-4}–3×10^{-4}	0.0114(6)	5.77×10^{-4}–8×10^{-4}	0.0096
1.0	0.0172(8)	0.0026	0.0152(6)	0.0041	0.0119
1.1	0.0155(10)	0.009	0.0149(4)	0.0108	0.0145
1.2	0.0147(10)	0.0125	0.0166(5)	0.0154	0.0172
1.3	0.00994(110)	0.0192	0.0151(20)	0.0210	0.0199
1.4	0.0142(20)	0.0245	0.00965(40)	0.0204	0.0227
1.5	0.0080(25)	0.0260	0.00683(20)	0.0188	0.0253

[a]Calculations use 108 h-wave functions for the T-matrix calculations. Amplitudes are obtained from seven-point quadratures using the first fourteen moments of $x=(E-S2)/(E+S2)$ for at least five different $S2$. Column DL represents our calculations using the Dalgarno-Lynn potential. Probably uncertainty in the imaginary part is less than ±7%.

[b]See Table I.

included most terms with $M \leq 8$ were carried out with the largest power of positron-electron coordinate including being r_{12}^3. The results are shown in Table VII. Extra static-type functions were included in an attempt to get more eigenvalues at higher energies above $E=4$–5; however, these static functions did not introduce many higher eigenvalues indicating lack of coupling with correlation functions. β was then increased to the value $\beta=1.2$ which spread the eigenvalues out toward larger energies. This greatly decreased the number of eigenvalues below $E=0.75$ hartrees, increasing the low-energy relative error.

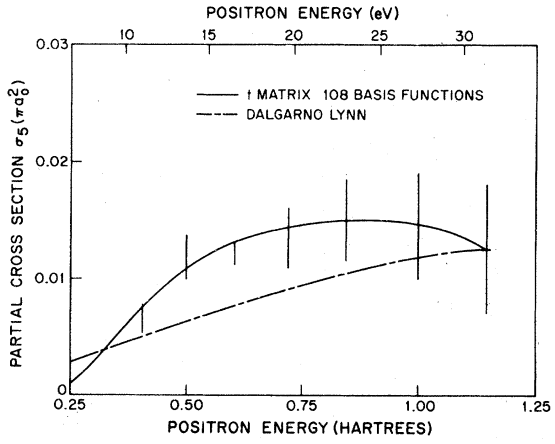

FIG. 6. h-wave ($L=5$) elastic partial cross section. The solid line is the result of the T-matrix calculations with 108 basis functions for $\beta=0.9$, 1.2. The bars indicate the possible error, an estimate obtained from the deviation of the different calculations. The broken curve (— - —) is the Dalgarno-Lynn result. Note the small size of the cross section, and that the moment T-matrix result is approaching the Dalgarno-Lynn.

The very small amplitudes obtained from the two calculations often differ by a large amount relative to their size. However, the absolute error is not any larger than that for previous partial waves. These results combine to give a very small elastic h-wave cross section which is shown

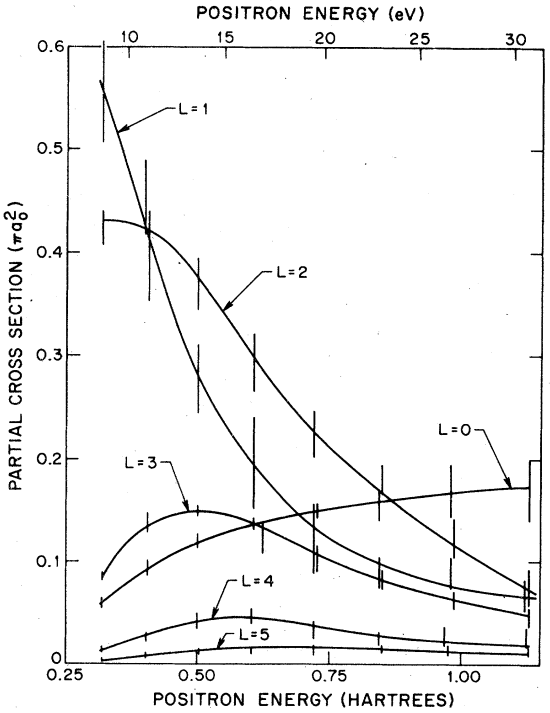

FIG. 7. Partial e^+-H elastic cross sections for $L=0$ through $L=5$. The contributions from $L=0$ to 3 are fairly large and all are about the same size. The $L=4$ and $L=5$ cross sections are rapidly decreasing, presumably indicating the convergence of the partial-wave expansion.

in Fig. 6. As seen in Fig. 6 the results are not only small but quite well approximated by the Dalgarno-Lynn elastic amplitude.

B. Elastic and total cross sections

The partial-wave contributions to the elastic $e^+ - H$ cross section over the range 8–30 eV are shown in Fig. 7. The $L=5$ results are quite small, indicating convergence of the partial-wave expansion. The converged elastic cross section calculated as the sum of partial cross sections for $L=0$ through 5 is shown in Fig. 8 where it is compared with the less well converged total cross section computed by assumption of unitarity, as discussed below. For comparison, the sum of the $L=6$ through 10 contributions to the Dalgarno-Lynn estimates of the elastic partial-wave amplitudes are shown and seem to be one and a half to two orders of magnitude smaller than the cross section computed from the first six partial waves, indicating quite reasonable convergence, considering the fairly optimistic estimate of 10% to 15% uncertainty in the cross section.

The total, or inclusive, cross section σ_{tot} for

$$e^+ + H \rightarrow \text{anything}$$

may be calculated from the elastic amplitude via the partial-wave optical theorem, $\sigma_{\text{tot}}^l = (4/k^2)(2l+1)\,\text{Im}(t_k^l)$, which follows from unitarity. Results for the partial-wave total cross sections are shown in Fig. 9 over the range 8–30 eV. It is evident that the errors in the partial-wave contributions are sizable, and that the total cross section

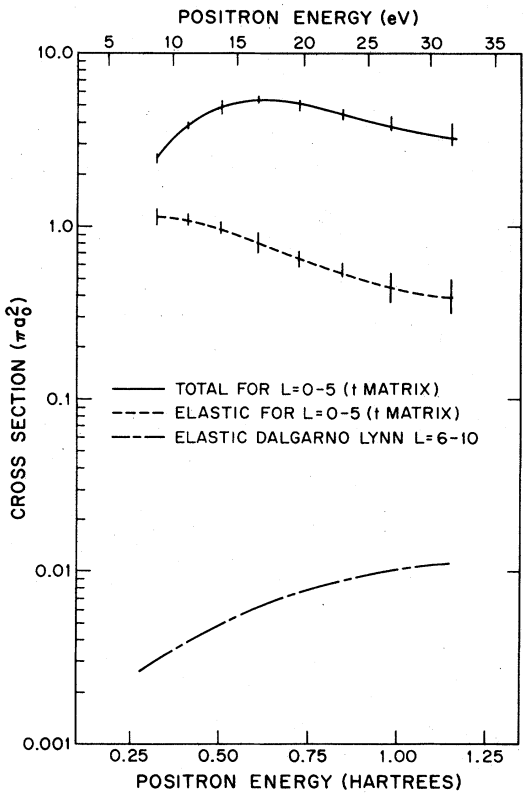

FIG. 8. Positron-hydrogen elastic cross section (---) calculated using the moment T-matrix values for partial waves $L=0$ through $L=5$ is shown to be much greater than the Dalgarno-Lynn contribution from partial waves $L=6$ through $L=10$. For such high angular momentum, we expect the Dalgarno-Lynn (— - —) to be a reasonable approximation, indicating good convergence of the elastic cross section. The solid curve represents the total (inclusive) cross section obtained by using the elastic T-matrix amplitudes for $L=0$ through $L=5$ and assuming unitarity.

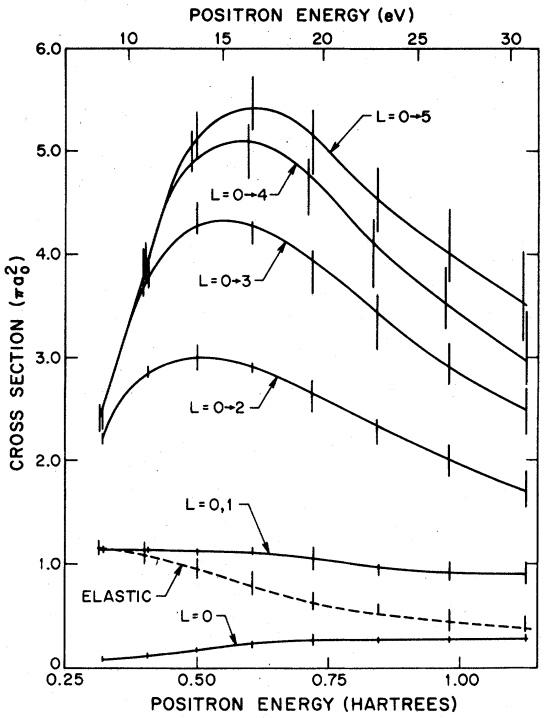

FIG. 9. Total positron-hydrogen cross section, e^+-H → anything. The estimates shown are based on the use of successively larger numbers of partial waves, up through a total of 6. The partial-wave cross sections are obtained from the elastic partial-wave amplitudes by application of the optical theorem, assuming unitarity. This is clearly an assumption: we have no way of testing whether unitarity is obeyed in this energy region, although it is satisfied at low energies. The cross section we obtain is not fully converged since there is still a noticeable difference between the estimates based on five and six partial waves. The $L=3$, 4, and 5 contributions are gradually getting smaller, but not at a very rapid rate. We can thus only put a lower bound (with the estimated errors) on the total cross section. The dashed line shows the converged (including partial waves $L=0$ through 5) elastic cross section (see Fig. 8).

is not fully converged. With the assumption that the partial-wave amplitudes are correct to the indicated accuracy, the total cross section should thus be considered as a lower bound to the true value. Additionally, it must be emphasized that as the computational methods used do not automatically enforce unitarity, use of the optical theorem to extract σ_{tot} from approximate elastic amplitudes is clearly an assumption. As a partial check, the elastic amplitudes extended into the purely elastic region below 0.25 a.u. (see T-matrix I) were found to satisfy *elastic* unitarity to within 1% or 2% in the worst cases, indicating that the assumption of overall unitarity is reasonable, but not constituting a demonstration of this fact for energies above the inelastic threshold.

III. SUMMARY

By direct construction of the discontinuity of the off-shell T-matrix elements $T_k(z)$, and by assuming unitarity, the elastic $e^+ - H$ partial-wave amplitudes and cross sections and total (inclusive) cross sections were computed over the energy region from 7 to 34 eV, in the intermediate-energy region above the pick-up and impact-ionization thresholds. The elastic cross section is converged over this whole energy range to within the error of the calculations, while the total cross section $e^+ + H \rightarrow$ anything, which is almost an order of magnitude larger than the elastic, is less well converged and should be taken to be a lower bound to the true total cross section.

ACKNOWLEDGMENTS

The support of the NSF through Grant Nos. CHE77-16307 and PHY76-04761, and Fellowship support (to W.P.R.) from the J. S. Guggenheim Memorial Foundation and the Council on Research and Creative Work of the University of Colorado, Boulder, are most gratefully acknowledged.

*Work completed while on leave from Dept. of Chemistry, Harvard University, Cambridge, Mass. 02138: Present address: Laboratory for Atmospheric and Space Physics, University of Colorado, Boulder, Colo. 80309.

[1]R. K. Peterkop, *Theory of Ionization of Atoms by Electron Impact*, translation edited by D. G. Hummer (Colorado Associated University, Boulder, Colo., 1977).

[2]L. Schlessinger and C. Schwartz, Phys. Rev. Lett. 16, 1173 (1966); L. Schlessinger, Phys. Rev. 167, 1411 (1968); 171, 1523 (1968).

[3]J. Nuttall and H. L. Cohen, Phys. Rev. 188, 1542 (1969).

[4]E. A. McDonald and J. Nuttall, Phys. Rev. Lett. 23, 361 (1969); G. Doolen, G. McCartor, E. A. McDonald, and J. Nuttall, Phys. Rev. A 4, 108 (1971).

[5]T. N. Rescigno and W. P. Reinhardt, Phys. Rev. A 10, 158 (1974).

[6]P. G. Burke and J. F. B. Mitchell, J. Phys. B 6, 320 (1973).

[7]J. Callaway and J. W. Wooten, Phys. Rev. A 9, 1924 (1974); J. Callaway and J. F. Williams, Phys. Rev. A 12, 2312 (1975).

[8]B. H. Bransden and M. R. C. McDowell, Phys. Rep. 30, 208 (1977).

[9]J. R. Winick and W. P. Reinhardt, preceding paper, Phys. Rev. A 18, 910 (1978) (referred to as T-matrix I).

[10]J. R. Winick, Ph.D. thesis (Harvard University, 1976) (unpublished).

[11]B. H. Bransden and Z. Jundi, Proc. Phys. Soc. Lond. 92, 880 (1967).

[12]M. F. Fels and M. H. Mittleman, Phys. Rev. 163, 129 (1967).

[13]J. F. Dirks and Y. Hahn, Phys. Rev. A 2, 1861 (1970); 3, 310 (1971).

[14]G. J. Seiler, R. S. Oberoi, and J. Callaway, Phys. Rev. A 3, 2006 (1971).

[15]S. E. A. Wakid and R. W. LaBahn, Phys. Rev. A 6, 2039 (1972).

[16]J. Stein and R. Sternlicht, Phys. Rev. A 6, 2165 (1972).

[17]Y. F. Chan and P. A. Fraser, J. Phys. B 6, 2504 (1973).

[18]Y. F. Chan and R. P. McEachran, J. Phys. B 9, 2869 (1976).

[19]A. K. Bhatia, A. Temkin, and H. Eiserike, Phys. Rev. A 9, 219 (1974).

[20]A. Dalgarno and H. Lynn, Proc. Phys. Soc. Lond. A 70, 223 (1957).